2021 19th International Symposium on Modeling and Optimization in Mobile, Ad hoc, and Wireless Networks (WiOpt)

Age of Information in Ultra-Dense Computation-Intensive Internet of Things (IoT) Systems

Bo Zhou*† and Walid Saad†
* College of Electronic and Information Engineering, Nanjing University of Aeronautics and Astronautics, Nanjing, China
† Wireless@VT, Bradley Department of Electrical and Computer Engineering, Virginia Tech, Blacksburg, VA, USA
Emails: {ecebo, walids}@vt.edu

***Abstract*—In this paper, a dense Internet of Things (IoT) monitoring system for computational intensive applications is studied in which a large number of devices with computing capability pre-process the collected raw status information into update packets and contend for transmitting them to the corresponding receivers, using a carrier sense multiple access (CSMA) scheme. Depending on whether the pre-processing operation completes when each device senses a channel, two policies are considered: *pre-process-then-Sense policy (PtS)* and *pre-processing-while-Sensing policy (PwS)*. Particularly, under policy PtS, each device must complete the pre-processing operation before sensing a channel; while under policy PwS, it performs the pre-processing operation and senses a channel concurrently. Here, for policy PwS, if the pre-processing operation is incomplete while a sensed channel is available to be used, then each device will still occupy the channel by sending dummy bits. For both policies, the closed-form expressions of the average age of information (AoI) are characterized. Then, a mean-field approximation framework with guaranteed accuracy is developed to study the asymptotic performance for the considered system in the large population regime. Simulation results validate the analytical results and show that the proposed mean-field approximation under policy PtS is accurate even for a small number of devices. It is also observed that policy PtS achieves a smaller average AoI than policy PwS, revealing that it is unnecessary for each device to occupy the channel before the pre-processing operation completes.**

I. Introduction

The proliferation of the Internet of Things (IoT) devices with advanced computing capabilities has significantly boosted the development of various real-world IoT applications, such as autonomous driving, smart surveillance, and predictive maintenance [1]. For these real-time applications, the time-sensitive status packet (e.g., an image) of the underlying physical process of interest collected by the IoT device requires certain computation-intensive data processing operations (e.g., image recognition) to extract the embedded status information. Thus, to maintain the freshness of the status information of the physical process at the destination for effective monitoring and control, it is imperative to take into account the data processing operations of the status packets.

Recently, there has been increasing attention on the analysis and optimization of the freshness of status information for computation-intensive IoT applications [2]–[9]. In these works, such freshness is quantified using the concept of *the age of information (AoI)*, which is defined as the time elapsed since the generation of the most recently status information received at the destination [10], [11]. In particular, the works in [2]–[4] analyze the AoI performance for computation-intensive status update systems with one device and one destination. The authors in [5] derive the moment generation function of the AoI for a computation-intensive status update system with two sources and one destination. The work in [6] proposes an optimal sampling and processing offloading policy to minimize the average age of processing for computation-intensive IoT monitoring system with one device and one destination. In [7], the authors analyze and minimize the average peak AoI for a computing-enabled IoT system with one data aggregator equipped with multiple sources, and one destination. The works in [8] and [9] study the average AoI for timely cloud computing, where the status packets collected by one device must be first processed at cloud servers and then sent back to the device.

In the existing literature on the analysis and optimization of the AoI for computation-intensive IoT applications, e.g. [2]–[9], there is either one source (one device or one data aggregator) or two sources. Note that, as next generation IoTs will encompass a large number of IoT devices [12], it is of great importance to investigate the AoI performance for ultra-dense computation-intensive IoT systems. The key challenges for such analysis involve the characterization of the complex temporal evolution of the AoI under data processing operations and the strong coupling among a large number of devices while accessing the channels and processing the status packets. Although a few works have studied the AoI in large-scale IoTs, e.g., [13]–[17], they did not consider data processing operations for the status packets, and, thus, are not applicable for computation-intensive IoT systems. To date, the AoI performance remains unknown for ultra-dense IoT systems for computation-intensive applications.

The main contribution of this work is, thus, a rigorous analytical characterization of the average AoI for an ultra-dense computation-intensive IoT system under a carrier sense multiple access (CSMA) type random access scheme. In particular, each device with computing capability needs to pre-process the collected raw status information to extract the embedded information into an update packet. Depending on whether an update packet is available when the device senses a channel under CSMA, we consider two policies:

This work was supported by the Office of Naval Research (ONR) under MURI Grant N00014-19-1-2621.

ISBN 978-3-903176-37-9 © 2021 IFIP

pre-process-then-Sense policy (PtS) and *pre-processing-while-Sensing policy (PwS)*. Under policy PtS, each device must complete the pre-processing operation to obtain an update packet before sensing a channel, while under policy PwS, each device can perform the pre-processing operation and sense a channel at the same time. Here, under policy PwS, if the pre-processing operation is not completed when the sensed channel is available to be used, the device will still occupy the channel and send dummy bits.

By using the technique of *stochastic hybrid systems (SHS)* [18], we characterize the closed-form expressions of the average AoI of each device for policies PtS and PwS under a given stationary distribution of the system. Then, we analyze the asymptotic performance of the two policies for our system in the large population regime using a mean-field approximation [19]–[21]. Simulation results validate our analytical results and show that the proposed mean-field approximation is very accurate for policy PtS even for a small number of devices. Moreover, we observe that policy PtS achieves a smaller average AoI compared with policy PwS. This indicates that it is not necessary to occupy the channel before the embedded information is extracted from the raw data.

II. System Model

As illustrated in Fig. 1, consider a real-time ultra-dense IoT monitoring systems for computation-intensive applications, composed of N pairs of identical IoT devices with computing capability and the associated receivers, and M identical wireless orthogonal channels. Let $\gamma \triangleq N/M \geq 1$. Each IoT device monitors the real-time status of the associated underlying physical process, for which the sensed raw status information requires certain pre-processing operations (e.g. initial feature extraction and pre-classification) before being transmitted to the receiver. Thus, we consider that each device encompasses a computation server to first pre-process the sensed raw data (referred to as *a computation packet*) and a transmitter to send the processed packet (referred to as *an update packet*) to the corresponding receiver afterwards. We consider that the computation packet of each underlying physical process arrives randomly at each device, following a Poisson process of rate λ. As in [5], we adopt a blocking packet management scheme, under which when the device is busy either pre-processing or transmitting, any arriving computation packets will be blocked and dropped.[1] We assume that for each device, the pre-processing time for each computation packet is exponentially distributed with mean $1/p$, as commonly done in prior art [3]–[5]. We further assume that each device can at most occupy one channel and the transmission time for each update packet over each channel is exponentially distributed with mean $1/\mu$.

We consider a CSMA-type random access scheme, under which each device senses the channels before transmitting its update packets. Note that, each device needs to first pre-process the computation packet and then transmit the update packet. Depending on whether an update packet is available when a device senses a channel, we consider two policies: *pre-process-then-Sense policy (PtS)* and *pre-processing-while-Sensing policy (PwS)*. In particular, under policy PtS, each device can only sense a channel when the pre-processing operation is completed; and under policy PwS, each device can sense a channel and pre-process the computation packet concurrently.

[1]The schemes with preemption in computation and/or transmission are left for future work.

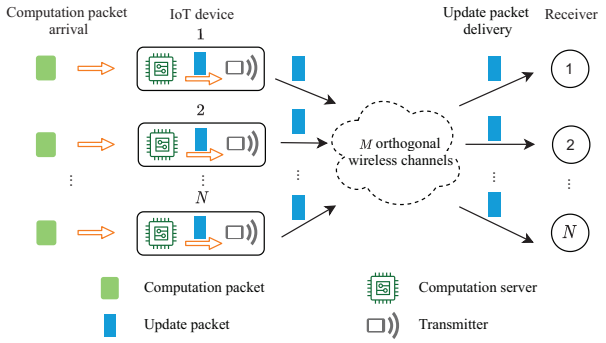

Fig. 1: Illustration of a real-time IoT monitoring system with N pairs of IoT devices with computing capability and their corresponding receivers, and M orthogonal wireless channels.

A. CSMA-Type Random Access for Policy PtS

Under policy PtS, for each device, there are four possible states: Idle (I), proprocessing (P), waiting (W), and transmitting (T). In particular, for a device in state I, if there is an arriving computation packet, then this device will move to state P to pre-process the computation packet so as to obtain an update packet. Then, prior to transmitting the update packet immediately (i.e., going to state T), as in [14]–[16], each device will randomly sense one of the channels to check whether it is occupied or not and move to state W. If the channel is sensed to be occupied, then the device remains silent; otherwise, the device still needs to wait for a random period of time, that is exponentially distributed with rate w. While waiting, the device keeps sensing the channel to identify any conflicting transmissions. If any such transmission is spotted, the device will stop its waiting timer and resume it when the channel is sensed idle. We adopt idealized CSMA assumptions, i.e., channel sensing is instantaneous and there are no hidden nodes, as commonly done in the literature [17], [22], [23]. Thus, the probability that multiple devices transmit their packets over any given channel concurrently is zero.

Next, we describe the state transitions of each device under policy PtS. Let $D_n(t) \in \mathcal{D} \triangleq \{I, P, W, T\}$ be the state of device n at time t. Then, let $X_d(t) \triangleq \frac{1}{N}\sum_{n=1}^{N} \mathbf{1}\left(D_n(t) = d\right)$ be the fraction of devices in state $d \in \mathcal{D}$ at t, where $\mathbf{1}(\cdot)$ is the indicator function. Let $\boldsymbol{X}(t) \triangleq (X_d(t))_{d\in\mathcal{D}}$. Note that, as all devices are exchangeable, we have $\mathbb{E}[X_d(t)] = \frac{1}{N}\sum_{n=1}^{N} \Pr[D_n(t) = d] = \Pr[D_n(t) = d]$ [19].

Under policy PtS, the state dynamics $\{D_n(t)\}$ of each device will be a continuous-time Markov chain (CTMC), as illustrate in Fig. 2(a). In particular, the device moves from state

ISBN 978-3-903176-37-9 © 2021 IFIP

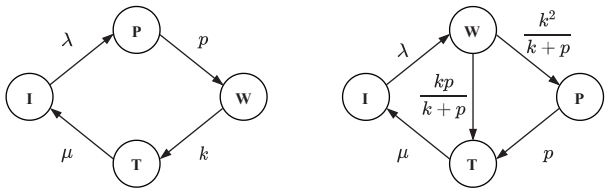

Fig. 2: Illustration of the state transition diagram of the CTMC of each device. (a) Policy PtS. $k = w(1 - \gamma X_T(t))$. (b) Policy PwS. $k = w(1 - \gamma(X_T(t) + X_P(t)))$.

I to state *P* when there is an arriving computation packet, which occurs with rate λ, and moves from state *P* to state *W* when the pre-process operation completes which occurs with rate p. When the device is in state *W*, the probability of finding an idle channel is $1 - \frac{1}{M}NX_T(t) = 1 - \gamma X_T(t)$. Thus, the transmission rate from from state *W* to state *T* is $w(1 - \gamma X_T(t))$, which is referred to as the effective rate k. Finally, the device moves from state *T* to state *I* with rate μ if it completes the transmission of one update packet.

B. CSMA-Type Random Access for Policy PwS

Under policy PwS, if a new computation packet arrives at an idle device, then the device starts to concurrently pre-process the computation packet and senses the channels in the same manner to that under policy PtS. When the device finishes the waiting period and successfully finds an idle channel, we consider that the device will immediately occupy the channel regardless whether the pre-processing operation is completed or not. Particularly, if the pre-processing operation is completed, then the device will transmit the obtained update packet; otherwise, the device keeps sending dummy bits until the pre-processing operation completes and an update packet is available. Here, the use of dummy bits is commonly adopted in the literature of CSMA (e.g., [17], [23] and [24]), which guarantees that the transmission over this particular channel can be identified by other devices so as to avoid transmission collisions. We can see that, under policy PwS, there are also four possible states for each device: idle (*I*), waiting while pre-processing (*W*), pre-processing while transmitting dummy bits (*P*), and transmitting the update packet (*T*).

Next, we describe the state transitions of each device under policy PwS. With abuse of notation, let $D_n(t)$ and $X_d(t)$ be the state of each device at t and the fraction of devices in state $d \in \mathcal{D} \triangleq \{I, W, P, T\}$ at t, respectively. Under policy PwS, the state dynamics $\{D_n(t)\}$ of each device is a CTMC, as illustrated in Fig. 2(b). In particular, the device moves from state *I* to state *W* when there is an arriving computation packet, which occurs with rate λ. When the device is in state *W*, the probability of finding an idle channel is $1 - \frac{1}{M}N(X_T(t) + X_P(t)) = 1 - \gamma(X_T(t) + X_P(t))$. Let Ψ be the event that the pre-processing operation completes within the waiting period and $\bar{\Psi}$ be its complement event. Note that, the waiting time T_w and the pre-processing time T_p are independently, exponentially distributed with parameters $k \triangleq w(1-\gamma(X_T(t)+X_P(t)))$ and p, respectively. Then, we can obtain the probabilities of the events Ψ and $\bar{\Psi}$, respectively, given by, $\Pr[\Psi] = \Pr[T_w > T_p] = \frac{p}{k+p}$ and $\Pr[\bar{\Psi}] = \frac{k}{k+p}$. Thus, the device moves from state *W* to state *T* and to state *P*, with rates $k\Pr[\Psi] = \frac{kp}{k+p}$ and $k\Pr[\bar{\Psi}] = \frac{k^2}{k+p}$, respectively. When the device is in state *P*, if the pre-processing operation completes, then it goes to state *T* with rate p. Finally, the device moves from state *T* to state *I* with rate μ.

C. Average AoI Metric

The status information carried in the computation packet starts aging as soon as the packet enters the computation server of each device. In this work, we adopt the AoI as the performance metric to quantify the freshness of the status information at the associated receiver of each device. At time t, if the most recently received update packet is timestamped $u(t)$, then the instantaneous AoI at the receiver is defined as $\Delta(t) = t - u(t)$ [10]. We are interested in deriving the average AoI of each device, given by $\bar{\Delta} \triangleq \lim_{\tau\to\infty} \frac{1}{\tau}\int_0^\tau \Delta(t)$, for the considered large-scale IoT system in the stationary regime under policies PtS and PwS. Let $\boldsymbol{\pi} \triangleq (\pi_d)_{d\in\mathcal{D}}$ be the stationary distribution of the CTMC of each device. From Fig. 2, it can be seen that the CTMCs are non-homogeneous with time-varying transition rates, for which it is generally impossible to calculate each corresponding stationary distribution. Thus, in the following, we will first analyze the average AoI of each device for both policies under a given stationary distribution, and then develop a mean-field approach to characterize the stationary distributions under the two policies for our system with a large number of devices.

III. Average AoI Analysis

In this section, we derive the expressions of the average AoI of each device under a given stationary distribution $\boldsymbol{\pi}$ for policies PtS and PwS. Note that, the traditional graphical approach for calculating the average AoI involves evaluating the correlations between the system times and the inter-arrival or inter-departure times. However, such a approach would be very challenging for the considered complex system in which the packets need to be pre-processed and wait before being transmitted. To avoid the challenge, we apply the SHS approach [18] to calculate the average AoI of each device. Next, we first briefly present the idea of the SHS approach for AoI analysis and the details can be found in [18].

A. Preliminaries of the SHS Approach

For AoI analysis, the SHS is modeled as a hybrid state $(q(t), \boldsymbol{z}(t))$, where $q(t) \in \mathcal{Q} = \{0, \cdots, Q\}$ is a finite-state CTMC that describes the occupancy of the system and $\boldsymbol{z}(t) = [z_0(t) \cdots z_n(t)] \in \mathcal{R}^{1\times(n+1)}$ describes the continuous-time evolution of age-related processes in the system. The CTMC $q(t)$ can be represented as a graph $(\mathcal{Q}, \mathcal{L})$ where each state $q \in \mathcal{Q}$ is a node and each transition $l \in \mathcal{L}$ is a directed edge $\triangleq (q_l, q_l')$ with transition rate $\lambda^{(l)}\delta_{q_l,q(t)}$. Here the Kronecker delta function $\delta_{q_l,q(t)}$ ensures that transition l occurs only when $q(t) = q_l$. When transition l occurs, the discrete state q_l jumps to q_l' and the continuous state $\boldsymbol{z}$

ISBN 978-3-903176-37-9 © 2021 IFIP

is reset to $\boldsymbol{z}' = \boldsymbol{z}\boldsymbol{A}_l$, where $\boldsymbol{A}_l \in \{0,1\}^{(n+1)\times(n+1)}$ is a binary transition reset map matrix. With each discrete state q, the continuous state $\boldsymbol{z}(t)$ evolves as the differential equation $\dot{\boldsymbol{z}}(t) = \boldsymbol{b}_q$. Here, $\boldsymbol{b}_q \triangleq [b_{q,0} \cdots b_{q,n}] \in \{0,1\}^{1\times(n+1)}$ is a binary vector where $b_{q,j}$ equals to 1 if $z_j(t)$ grows at a unit rate in state q and $b_{q,j}$ equals to 0 if $z_j(t)$ is irrelevant in state q and does not need to be tracked.

Let $\mathcal{L}'_q \triangleq \{l \in \mathcal{L} : q'_l = q\}$ and $\mathcal{L}_q \triangleq \{l \in \mathcal{L} : q_l = q\}$ be, respectively, the set of incoming and outgoing transitions for each state q. According to [18, Theorem 4], if the CTMC $q(t)$ is ergodic with stationary distribution $\boldsymbol{\pi} \triangleq [\pi_0 \cdots \pi_Q]$ and we can find a non-negative vector $\boldsymbol{v} \triangleq [\boldsymbol{v}_0 \cdots \boldsymbol{v}_Q]$ such that

$$\boldsymbol{v}_q \sum_{l\in\mathcal{L}_q} \lambda^{(l)} = \boldsymbol{b}_q \pi_q + \sum_{l\in\mathcal{L}'_q} \lambda^{(l)} \boldsymbol{v}_{q_l} \boldsymbol{A}_l, \forall q \in \mathcal{Q}, \tag{1}$$

then the average AoI is given by

$$\bar{\Delta} = \sum_{q\in\mathcal{Q}} v_{q0}. \tag{2}$$

B. Characterization of Average AoI

We now use the SHS approach to derive the expressions of the average AoI of each device for our considered system under a given stationary distribution for policies PtS and PwS.

1) Policy PtS: We begin with policy PtS. To use the SHS approach, we model the state of each device of our system under policy PtS with the discrete state $q(t) \in \mathcal{Q} = \{0,1,2,3\}$, where 0, 1, 2, and 3 indicate states *I*, *P*, *W*, and *T*, respectively. The continuous state for this system is $\boldsymbol{z}(t) = [z_0(t)\ z_1(t)]$, where $z_0(t)$ is the current AoI $\Delta(t)$ at the associated receiver for the device and $z_1(t)$ is the age of the packet at the device, when there is either a computation packet being pre-processed or an update packet in waiting or in service, otherwise $z_1(t)$ is irrelevant and is set to 0. Here, we would like to emphasize that there is no need to differentiate the age of the computation packet and the age of the update packet, and, thus, the calculations for using the SHS approach can be greatly reduced. With abuse of notation, let $k = w(1-\gamma\pi_T)$ be the effective waiting rate under the stationary distribution $\boldsymbol{\pi}$ for policy PtS. We illustrate the SHS Markov chain of $q(t)$ in Fig. 3 and summarize the corresponding transitions in Table I, which are further explained in the following.

- $l = 1$: A computation packet arrives at the device in state *I*, which occurs with rate λ. With this arrival, $z'_0 = z_0$ remains unchanged as it does not yield an AoI reduction at the receiver. Since the arriving arriving computation packet is fresh and its age is zero, we have $z'_1 = 0$.
- $l = 2$: The device completes the pre-processing operation of the computation packet at a rate of p and starts to sense one of the channels. In this transition, the AoI at the receiver remains the same, i.e., $z'_0 = z_0$. Although the computation packet becomes the update packet, the age of the packet currently at the device remains the same.
- $l = 3$: The device finds an idle channel and finishes the waiting period with rate k. This does not change the AoI at the receiver nor the age of the device's current packet. Thus, we have $z'_0 = z_0$ and $z'_1 = z_1$.

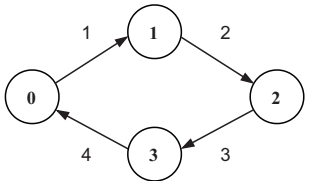

Fig. 3: Illustration of the SHS Markov chain under policy PtS.

- $l = 4$: The device completes its transmission service at a rate of μ. With this transition, the AoI at the receiver is reset to the age of the packet at the device that is delivered, i.e., $z'_0 = z_1$. Since there is no packet at the device, z'_1 is irrelevant, and, thus, is set to zero.

For the differential equation governing the evolution of the age-related processes $\boldsymbol{z}(t)$, it can be seen that the AoI at the receiver $\Delta(t) = z_0(t)$ always increases at a unit rate with time t in all the discrete states, i.e., $\dot{z}_0(t) = 1, \forall q \in \mathcal{Q}$. On the contrary, the age of the packet at the device $z_1(t)$ increases at a unit rate in state $q = 1,2,3$ in which there is either a computation packet or an update packet at the device. Thus, the evolution of $\boldsymbol{z}(t)$ depends on the discrete state $q(t)$. In particular, when $q(t) = q$, we have

$$\dot{\boldsymbol{z}}(t) = \boldsymbol{b}_q = \begin{cases} [1\ 0], & \text{if } q = 0, \\ [1\ 1], & \text{if } q = 1,2,3. \end{cases} \tag{3}$$

From Fig. 3, the stationary distribution $\boldsymbol{\pi}$ of $q(t)$ satisfies the following detailed balance equations:

$$\lambda\pi_0 = p\pi_1 = k\pi_2 = \mu\pi_3, \tag{4a}$$

$$\pi_0 + \pi_1 + \pi_2 + \pi_3 = 1. \tag{4b}$$

Then, we have:

$$\boldsymbol{\pi} = [\pi_0\ \pi_1\ \pi_2\ \pi_3] = \frac{1}{\frac{1}{\lambda}+\frac{1}{p}+\frac{1}{k}+\frac{1}{\mu}} \left[\frac{1}{\lambda}\ \frac{1}{p}\ \frac{1}{k}\ \frac{1}{\mu}\right]. \tag{5}$$

Next, we calculate $\boldsymbol{v} = [v_{00}\ v_{01}\ v_{10}\ v_{11}\ v_{20}\ v_{21}\ v_{30}\ v_{31}]$ in (1). By Table I and (3), we have

$$\lambda[v_{00}\ v_{01}] = \pi_0[1\ 0] + \mu[v_{31}\ 0], \tag{6a}$$

$$p[v_{10}\ v_{11}] = \pi_1[1\ 1] + \lambda[v_{00}\ 0], \tag{6b}$$

$$k[v_{20}\ v_{21}] = \pi_2[1\ 1] + p[v_{10}\ v_{11}], \tag{6c}$$

$$\mu[v_{30}\ v_{31}] = \pi_3[1\ 1] + k[v_{20}\ v_{21}]. \tag{6d}$$

According to (2), after complex calculations of (6), we can obtain the closed-form expression of the average AoI of each device for our system under the stationary distribution $\boldsymbol{\pi}$ for policy PtS, given by $\bar{\Delta}_{\text{PtS}} = v_{00} + v_{01} + v_{11}$.

2) Policy PwS: Following the SHS approach for policy PtS, we next derive the expression of the average AoI of each device for our considered system under $\boldsymbol{\pi}$ for policy PwS. Similarly, to model the system under policy PwS using the SHS approach, the discrete state is $q(t) \in \mathcal{Q} = \{0,1,2,3\}$, where 0, 1, 2, and 3 indicate states *I*, *W*, *P*, and *T*, respectively, and the continuous state is $\boldsymbol{z}(t) = [z_0(t)\ z_1(t)]$, which is the same to that for policy PtS. With abuse of notation, let $k = w(1-\gamma(\pi_T(t)+\pi_P(t)))$ be the corresponding effective

ISBN 978-3-903176-37-9 © 2021 IFIP

TABLE I: Transitions for the SHS Markov chain under policy PtS in Fig. 3.

l	$q_l \to q_l'$	$\lambda^{(l)}$	$\boldsymbol{z}' = \boldsymbol{z}\boldsymbol{A}_l$	$\boldsymbol{A}_l$	$\boldsymbol{v}_{q_l}\boldsymbol{A}_l$
1	$0 \to 1$	λ	$[z_0 \;\; 0]$	$\begin{bmatrix}1&0\\0&0\end{bmatrix}$	$[\bar{v}_{00} \;\; 0]$
2	$1 \to 2$	p	$[z_0 \;\; z_1]$	$\begin{bmatrix}1&0\\0&1\end{bmatrix}$	$[\bar{v}_{10} \;\; \bar{v}_{11}]$
3	$2 \to 3$	k	$[z_0 \;\; z_1]$	$\begin{bmatrix}1&0\\0&1\end{bmatrix}$	$[\bar{v}_{20} \;\; \bar{v}_{21}]$
4	$3 \to 0$	μ	$[z_1 \;\; 0]$	$\begin{bmatrix}0&0\\1&0\end{bmatrix}$	$[\bar{v}_{31} \;\; 0]$

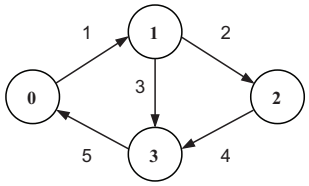

Fig. 4: Illustration of the SHS Markov chain under policy PwS.

waiting rate under $\boldsymbol{\pi}$. Then, the SHS Markov chain of $q(t)$ is illustrated in Fig. 3 and the corresponding transitions are summarized in Table I and explained below.

- $l = 1$: A computation packet arrives at the device in state *I*, which occurs with rate λ, and the device moves from state *I* to *W*. In this transition, $z_0' = z_0$ remains unchanged and $z_1' = 0$ because the packet is fresh.
- $l = 2$: The device finishes the waiting period and goes to state *P* if the processing operation is not completed, which occurs with rate $\frac{k^2}{k+p}$. In this transition, the AoI at the receiver remains unchanged, i.e., $z_0' = z_0$. As the device is still pre-processing the computation packet, no age reduction occurs for the packet currently at the device, i.e., $z_1' = z_1$.
- $l = 3$: The device finishes the waiting period and goes to state *T* if the processing operation is completed, which occurs with rate $\frac{kp}{k+p}$. This does not change the AoI at the receiver, i.e., $z_0' = z_0$. Although the computation packet becomes the update packet, the age of the packet currently at the device remains unchanged, i.e., $z_1' = z_1$.
- $l = 4$: The device completes the pre-processing operation of the computation packet at a rate of p and starts to transmit the update packet instead of the dummy bits. However, this does not change the AoI at the receiver nor the age of the device's current packet.
- $l = 5$: The device completes its transmission with rate μ. The AoI at the receiver is reset to the age of the packet at the device that is delivered, i.e., $z_0' = z_1$. As there is no packet at the device, z_1' is set to zero.

It can be easily seen that, the evolution of $\boldsymbol{z}(t)$ under policy PwS is governed by the same differential equations as in (3). By Fig. 4 and Table II, the stationary distribution $\boldsymbol{\pi}$ of $q(t)$ satisfies the following system of linear equations:

$$\lambda\pi_0 = (\frac{k^2}{k+p} + \frac{kp}{k+p})\pi_1 = \mu\pi_3, \tag{7a}$$

$$\frac{k^2}{k+p}\pi_1 = p\pi_2, \tag{7b}$$

TABLE II: Transitions for the SHS Markov chain under policy PwS in Fig. 4.

l	$q_l \to q_l'$	$\lambda^{(l)}$	$\boldsymbol{z}' = \boldsymbol{z}\boldsymbol{A}_l$	$\boldsymbol{A}_l$	$\boldsymbol{v}_{q_l}\boldsymbol{A}_l$
1	$0 \to 1$	λ	$[z_0 \;\; 0]$	$\begin{bmatrix}1&0\\0&0\end{bmatrix}$	$[\bar{v}_{00} \;\; 0]$
2	$1 \to 2$	$\frac{k^2}{k+p}$	$[z_0 \;\; z_1]$	$\begin{bmatrix}1&0\\0&1\end{bmatrix}$	$[\bar{v}_{10} \;\; \bar{v}_{11}]$
3	$1 \to 3$	$\frac{kp}{k+p}$	$[z_0 \;\; z_1]$	$\begin{bmatrix}1&0\\0&1\end{bmatrix}$	$[\bar{v}_{10} \;\; \bar{v}_{11}]$
4	$2 \to 3$	p	$[z_0 \;\; z_1]$	$\begin{bmatrix}1&0\\0&1\end{bmatrix}$	$[\bar{v}_{20} \;\; \bar{v}_{21}]$
5	$3 \to 0$	μ	$[z_1 \;\; 0]$	$\begin{bmatrix}0&0\\1&0\end{bmatrix}$	$[\bar{v}_{31} \;\; 0]$

$$\frac{kp}{k+p}\pi_1 + p\pi_2 = \mu\pi_3, \tag{7c}$$

$$\pi_0 + \pi_1 + \pi_2 + \pi_3 = 1. \tag{7d}$$

Then, we have:

$$\begin{aligned}\boldsymbol{\pi} &= [\pi_0 \;\; \pi_1 \;\; \pi_2 \;\; \pi_3] \\ &= \frac{1}{\frac{1}{\lambda} + \frac{k}{(k+p)p} + \frac{1}{k} + \frac{1}{\mu}} \left[\frac{1}{\lambda} \;\; \frac{1}{k} \;\; \frac{k}{(k+p)p} \;\; \frac{1}{\mu}\right].\end{aligned} \tag{8}$$

Then, according to (2), we can calculate the average AoI of each device under $\boldsymbol{\pi}$ for policy PwS as $\bar{\Delta}_{\text{PwS}} = v_{00} + v_{01} + v_{11}$, where v_{00}, v_{01} and v_{11} satisfy the following linear system of equations by (1):

$$\lambda[v_{00} \;\; v_{01}] = \pi_0[1 \;\; 0] + \mu[v_{31} \;\; 0], \tag{9a}$$

$$(\frac{k^2}{k+p} + \frac{kp}{k+p})[v_{10} \;\; v_{11}] = \pi_1[1 \;\; 1] + \lambda[v_{00} \;\; 0], \tag{9b}$$

$$p[v_{20} \;\; v_{21}] = \pi_2[1 \;\; 1] + \frac{k^2}{k+p}[v_{10} \;\; v_{11}], \tag{9c}$$

$$\mu[v_{30} \;\; v_{31}] = \pi_3[1 \;\; 1] + \frac{kp}{k+p}[v_{10} \;\; v_{11}] + p[v_{20} \;\; v_{21}]. \tag{9d}$$

Next, we summarize the closed-form expressions of the average AoI of each device for policies PtS and PwS.[2]

Theorem 1: Under the stationary distribution $\boldsymbol{\pi}$, for each device, the average AoI under policies PtS and PwS are, respectively, given as follows:

$$\begin{aligned}\bar{\Delta}_{\text{PtS}} =& \frac{1}{\lambda} + \frac{1}{k} + \frac{2}{\mu} + \frac{1}{p} \\ &+ \frac{1}{\frac{1}{\lambda} + \frac{1}{p} + \frac{1}{k} + \frac{1}{\mu}} \left(\frac{1}{p^2} + \frac{1}{k^2} + \frac{1}{pk} - \frac{1}{\lambda\mu}\right),\end{aligned} \tag{10}$$

$$\begin{aligned}\bar{\Delta}_{\text{PwS}} =& \frac{1}{\lambda} + \frac{1}{k} + \frac{2}{\mu} + \frac{k}{p(k+p)} + \frac{1}{\frac{1}{\lambda} + \frac{k}{(k+p)p} + \frac{1}{k} + \frac{1}{\mu}} \times \\ &\left(\frac{1}{k^2} + \frac{1}{p(k+p)} + \frac{k}{p^2(k+p)} - \frac{1}{\lambda\mu}\right).\end{aligned} \tag{11}$$

From Theorem 1, we can see that in the limiting case with both the computation rate p and the effective waiting rate k going to infinity (i.e., the device can obtain an update packet and transmit it upon immediately upon a new computation packet arrives), the average AoI for both polices are given by

$$\lim_{p,k\to\infty} \bar{\Delta}_{\text{PtS}} = \lim_{p,k\to\infty} \bar{\Delta}_{\text{PwS}} = \frac{1}{\lambda} + \frac{2}{\mu} - \frac{1}{\lambda+\mu}, \tag{12}$$

[2]All proofs are omitted due to space limitations.

ISBN 978-3-903176-37-9 © 2021 IFIP

which is the same to the average AoI in an FCFS M/M/1/1 queue [25]. Moreover, in the limiting case with the computation rate p going to infinity, we can see that policy PtS is equivalent to policy PwS with the same average AoI. Note that, we cannot directly compare the average AoI between policies PtS and PwS, based on the closed-form expressions under a given stationary distribution in Theorem 1. This is because that the stationary distributions of the two policies would be different under the same system parameters, which can be seen from the CTMCs in Figs. 2(a) and 2(b). We will compare the average AoI for the two policies in the simulations. Theorem 1 provides rigorous analytical characterizations of the average AoI of each device for policies PtS and PwS under a given stationary distribution $\boldsymbol{\pi}$. Next, we analyze $\boldsymbol{\pi}$ under the two policies for our system in an ultra-dense regime with a large number of devices by a mean-field approximation [19]–[21].

IV. Mean-Field Analysis for Dense IoTs

As mentioned earlier, it is generally impossible to calculate the stationary distribution $\boldsymbol{\pi}$ of the CTMCs in Fig. 2 for the considered system with a large number of devices, because of the resulting large state space, and the non-linear and time-varying transition rates [26]. Consequently, we adopt a mean-field approach to characterize $\boldsymbol{\pi}$ under policies PtS and PwS for our system in the mean-field regime in which, the number of the devices N goes to infinity and the number of channels M scales with N according to $M = N/\gamma$.

A. Mean-Field Analysis for Policy PtS

Under policy PtS, recall that $\boldsymbol{X}(t) \triangleq (X_d(t))_{d\in\mathcal{D}}$ is the fraction of devices in each state $d \in \mathcal{D}$ at t. Then, by Fig. 2(a), the random process $\{\boldsymbol{X}(t), t \geq 0\}$ for a finite N is a Markov process with the state space $\{0, \frac{1}{N}, \cdots, \frac{N-1}{N}, 1\}^4$ and the following transition rates:

$$\begin{cases} \boldsymbol{X} \mapsto \boldsymbol{X} + \frac{1}{N}(-1,1,0,0) & \text{at rate } N\lambda X_I, \\ \boldsymbol{X} \mapsto \boldsymbol{X} + \frac{1}{N}(0,-1,1,0) & \text{at rate } NpX_P, \\ \boldsymbol{X} \mapsto \boldsymbol{X} + \frac{1}{N}(0,0,-1,1) & \text{at rate } Nw(1-\gamma X_T)X_W, \\ \boldsymbol{X} \mapsto \boldsymbol{X} + \frac{1}{N}(1,0,0,-1) & \text{at rate } N\mu X_T. \end{cases} \tag{13}$$

The form of the transitions in (13) indicates that $\{\boldsymbol{X}(t), t \geq 0\}$ is a density-dependent population process [19] and the corresponding mean-field model ($N \to \infty$) can be characterized by the following ordinary differential equation (ODE):

$$\dot{\boldsymbol{x}} = f(\boldsymbol{x}) = \lim_{dt\to 0} \frac{\mathbb{E}[\boldsymbol{X}(t+dt) - \boldsymbol{X}(t) \mid \boldsymbol{X}(t) = \boldsymbol{x}]}{dt}, \tag{14}$$

where $\boldsymbol{x} \triangleq (x_I, x_P, x_W, x_T)$. From (13), we have

$$\begin{cases} \dot{x}_I = -\lambda x_I + \mu x_T, \\ \dot{x}_P = \lambda x_I - p x_P, \\ \dot{x}_W = p x_P - w(1-\gamma x_T)x_W, \\ \dot{x}_T = w(1-\gamma x_T)x_W - \mu x_T. \end{cases} \tag{15}$$

Then, by proving that the function $f(\boldsymbol{x})$ is Lipschitz continuous, and the mean-field model in (15) is locally exponentially stable and globally asymptotically stable, we can show the following theorem.

Theorem 2: Under policy PtS, the mean-field model in (15) is accurate for the considered system in both the transient and stationary regimes.

1) For the transient regime with a finite time horizon $[0, T]$, if the initial state $\boldsymbol{X}(0) \to \boldsymbol{x}_0 \in [0,1]^4$ as $N \to \infty$ almost surely, then for any $T > 0$, we have

$$\lim_{N\to\infty} \sup_{t\leq T} \|\boldsymbol{X}(t) - \boldsymbol{x}(t)\| = 0, \text{almost surely}, \tag{16}$$

where $\boldsymbol{x}(t)$ is the solution to the ODE in (15) with $\boldsymbol{x}(0) = \boldsymbol{x}_0$.

2) For the stationary regime with $T \to \infty$, the stationary distribution $\boldsymbol{\pi}$ of the CTMC $\{\boldsymbol{X}(t), t \geq 0\}$ converges weakly to $\boldsymbol{x}^*$ as $N \to \infty$ with the rate of convergence:

$$|\mathbb{E}[\boldsymbol{\pi}] - \boldsymbol{x}^*| = O(\frac{1}{N}), \tag{17}$$

where $\boldsymbol{x}^*$ is the unique equilibrium point of the mean-field model in (14) and is given by:

$$x_I^* = \frac{\mu}{\lambda}x_T^*,\ x_P^* = \frac{\mu}{p}x_T^*,\ x_W^* = \frac{\mu x_T^*}{w(1-\gamma x_T^*)},$$
$$x_T^* = \frac{1}{2w\gamma(\frac{1}{\mu}+\frac{1}{\lambda}+\frac{1}{p})}\Bigg(w(\frac{1+\gamma}{\mu}+\frac{1}{\lambda}+\frac{1}{p})+1 - \sqrt{\left(w(\frac{1+\gamma}{\mu}+\frac{1}{\lambda}+\frac{1}{p})+1\right)^2 - \frac{4w^2\gamma}{\mu}(\frac{1}{\mu}+\frac{1}{\lambda}+\frac{1}{p})}\Bigg).$$

Moreover, the average AoI $\bar{\Delta}_{\text{PtS}}(\boldsymbol{\pi})$ converges weakly to $\bar{\Delta}_{\text{PtS}}(\boldsymbol{x}^*)$ with the rate of convergence:

$$\left|\mathbb{E}[\bar{\Delta}_{\text{PtS}}(\boldsymbol{\pi})] - \bar{\Delta}_{\text{PtS}}(\boldsymbol{x}^*)\right| = O(\frac{1}{N}). \tag{19}$$

In (17) and (19), the expectation is taken over the stationary distribution $\boldsymbol{\pi}$ for the system with finite N.

B. Mean-Field Analysis for Policy PwS

Similar to that for policy PtS, by Fig. 2(b), we know that, for a finite N, the CTMC $\{\boldsymbol{X}(t), t \geq 0\}$ under policy PwS is a density-dependent population process with the following transition rates:

$$\begin{cases} \boldsymbol{X} \mapsto \boldsymbol{X} + \frac{1}{N}(-1,1,0,0) & \text{at rate } N\lambda X_I, \\ \boldsymbol{X} \mapsto \boldsymbol{X} + \frac{1}{N}(0,-1,1,0) & \text{at rate } N\frac{w^2(1-\gamma(X_P+X_T))^2}{w(1-\gamma(X_P+X_T))+p}X_W, \\ \boldsymbol{X} \mapsto \boldsymbol{X} + \frac{1}{N}(0,-1,0,1) & \text{at rate } N\frac{w(1-\gamma(X_P+X_T))p}{w(1-\gamma(X_P+X_T))+p}X_W, \\ \boldsymbol{X} \mapsto \boldsymbol{X} + \frac{1}{N}(0,0,-1,1) & \text{at rate } NpX_P, \\ \boldsymbol{X} \mapsto \boldsymbol{X} + \frac{1}{N}(1,0,0,-1) & \text{at rate } N\mu X_T. \end{cases} \tag{20}$$

ISBN 978-3-903176-37-9 © 2021 IFIP

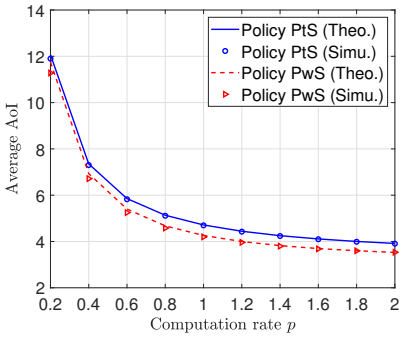

Fig. 5: Average AoI versus the computation rate p under a given stationary distribution. $\lambda = 1, \mu = 1$, and $k = 2$.

Then, we can characterize the corresponding mean-field model ($N \to \infty$) by $\dot{\boldsymbol{x}} = f(\boldsymbol{x})$, where $\boldsymbol{x} \triangleq (x_I, x_W, x_P, x_T)$ and

$$\begin{cases} \dot{x}_I = -\lambda x_I + \mu x_T, \\ \dot{x}_W = \lambda x_I - w(1-\gamma(x_P+x_T))x_W, \\ \dot{x}_P = \dfrac{w^2(1-\gamma(x_P+x_T))^2}{w(1-\gamma(x_P+x_T))+p} x_W - p x_P, \\ \dot{x}_T = \dfrac{w(1-\gamma(x_P+x_T))p}{w(1-\gamma(x_P+x_T))+p} x_W + p x_P - \mu x_T. \end{cases} \tag{21}$$

Next, by proving that the function $f(\boldsymbol{x})$ is Lipschitz continuous, we show that the mean-field model in (21) is accurate for our system under policy PwS in the transient regime.

Theorem 3: Under policy PwS, if the initial state $\boldsymbol{X}(0) \to \boldsymbol{x}_0 \in [0,1]^4$ as $N \to \infty$ almost surely, then for any $T > 0$, we have

$$\lim_{N\to\infty} \sup_{t \le T} \|\boldsymbol{X}(t) - \boldsymbol{x}(t)\| = 0, \text{almost surely}, \tag{22}$$

where $\boldsymbol{x}(t)$ is the solution to the ODE in (21) with $\boldsymbol{x}(0) = \boldsymbol{x}_0$.

Note that, for policy PwS, due to the complex terms in (21), we are not able to prove the locally exponentially stability and globally asymptotically stability of the mean-field model. Thus, the convergence results for the stationary regime as in Theorem 2 could not be shown theoretically for policy PwS.

V. Simulation Results and Analysis

We now present numerical results to illustrate the average AoI for policies PtS and PwS under a given stationary distribution in Theorem 1, the accuracy of the mean-field approximation in Theorems 2 and 3, and the average AoI achieved by the two policies in the mean-field limit.

In Fig. 5, we provide the analytical results obtained in Theorem 1 and the simulation results obtained by averaging over 50,000 computation packet arrivals, for the average AoI under policies PtS and PwS. We observe that the simulation results agree closely with the analytical results thus validating the closed-form expressions of the average AoI derived in Theorem 1. We also observe that, for a given effective waiting rate k, policy PwS achieves a smaller average AoI than policy PtS. However, this does not hold for the case in which the effective waiting rate k is not fixed and depends on the system parameters, as will be shown next.

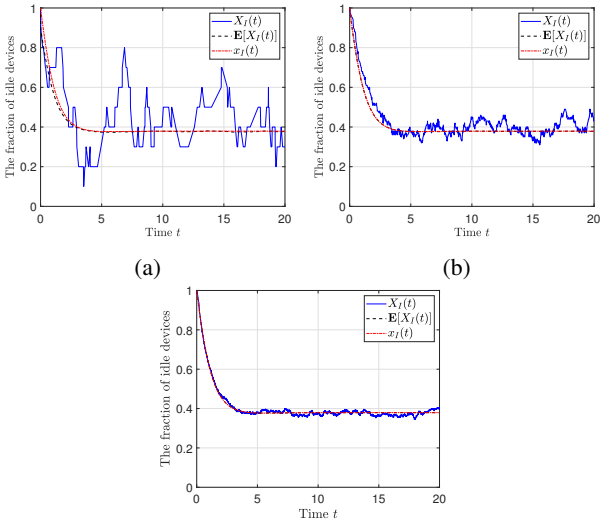

(a) (b) (c)

Fig. 6: The evolutions of the fraction of IoT devices in state I for the CTMC $\boldsymbol{X}(t)$ under policy PtS with various numbers of devices N. $\lambda = 0.8$, $\mu = 1.5$, $w = 2$, $\gamma = 5$, and $p = 0.8$. (a) $N = 10$. (b) $N = 100$. (c) $N = 1000$.

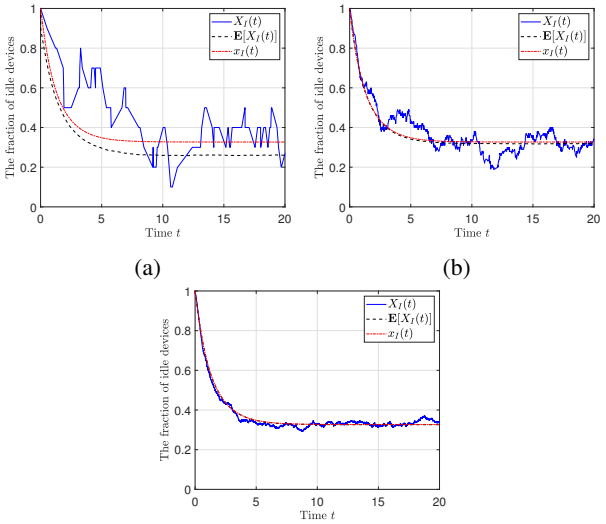

(a) (b) (c)

Fig. 7: The evolutions of the fraction of IoT devices in state I for the CTMC $\boldsymbol{X}(t)$ under policy PwS with various numbers of devices N. $\lambda = 0.8$, $\mu = 1.5$, $w = 2$, $\gamma = 5$, and $p = 0.8$.

Then, we simulate the considered system for population sizes of $N = 10$, $N = 100$, and $N = 1000$ of devices and illustrate the evolution of the fraction of devices in state I under policies PtS and PwS in Figs. 6 and 7, respectively. Each subfigure contains three curves: one simulation trajectory $X_I(t)$, the average of 10,000 runs of simulation trajectories $\mathbb{E}[X_I(t)]$, and the mean-field approximation $x_I(t)$. From Figs. 6 and 7, we can see that the simulation results of one trajectory converges $X_I(t)$ to the mean-field approximation $x_I(t)$ as N increases, under both polices PtS and PwS. Moreover, under policy PtS, from Fig. 6, we observe that the averaged simulation result $\mathbb{E}[X_I(t)]$ is very close to the

ISBN 978-3-903176-37-9 © 2021 IFIP

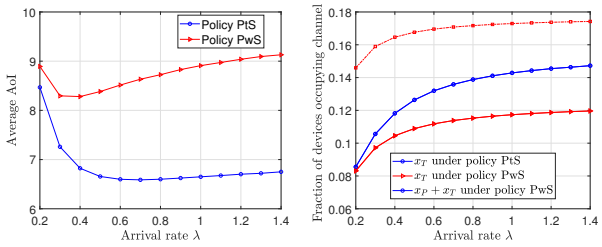

(a) (b)

Fig. 8: Performance comparison between policies PtS and PwS in the mean-field limit under varying arrival rates λ. $\mu = 1.5$, $w = 2$, $\gamma = 5$, and $p = 0.8$. (a) The average AoI. (b) The fraction of devices occupying the channels.

mean-field approximation $x_I(t)$, even when $N = 10$.

Finally, in Fig. 8, we show the average AoI and the fraction of devices occupying the channels achieved by policies PtS and PwS with difference arrival rates in the mean-field limit. From Fig. 8(a), surprisingly, we obverse that policy PtS achieves a smaller average AoI compared with policy PwS. This indicates that it is not necessary to occupy the channel before the pre-processing operation completes. The reason is that, under policy PwS, although the fraction of devices $x_P + x_T$ that are occupying the channels (i.e., transmitting dummy bits in state P or update packet in state T) is higher than x_T under policy PtS, there are fewer devices that are transmitting update packets compared with policy PtS, as shown in Fig. 8(b). Moreover, we observe that, for both policies, the average AoI first decreases and then increases with the arrival rate λ. This is because as λ increases, the effective waiting rate k decreases as there will be more devices occupying the channels.

VI. Conclusion

In this paper, we have studied the average AoI performance for a ultra-dense computation-intensive IoT monitoring system under a CSMA-type random access scheme. Depending on whether the pre-processing operation completes when sensing a channel under CSMA, we have considered two polices, i.e., policies PtS and PwS. For each policy, we have characterized the closed-form expressions of the average AoI of each device for a given stationary distribution of the system. Then, we have proposed a mean-field approximation approach to investigate the asymptotic performance of our considered system with a large number of devices. Simulation results corroborate the correctness of the derived expressions of the average AoI and shown that the mean-filed approximation is very accurate under policy PtS even for a small number of devices. Moreover, the results show that policy PtS achieves a smaller average AoI than policy PwS, indicating that it is unnecessary for a device to occupy a channel before completing the pre-processing operation.

References

[1] W. Saad, M. Bennis, and M. Chen, "A vision of 6G wireless systems: Applications, trends, technologies, and open research problems," *IEEE Netw.*, vol. 34, no. 3, pp. 134–142, May 2020.

[2] P. Zou, O. Ozel, and S. Subramaniam, "Optimizing information freshness through computation–transmission tradeoff and queue management in edge computing," *IEEE/ACM Trans. Netw.*, vol. 29, no. 2, pp. 949–963, 2021.

[3] Q. Kuang, J. Gong, X. Chen, and X. Ma, "Analysis on computation-intensive status update in mobile edge computing," *IEEE Trans. Veh. Technol.*, vol. 69, no. 4, pp. 4353–4366, 2020.

[4] F. Chiariotti, O. Vikhrova, B. Soret, and P. Popovski, "Peak age of information distribution for edge computing with wireless links," *IEEE Trans. Commun.*, 2021, to appear.

[5] M. Moltafet, M. Leinonen, and M. Codreanu, "Moment generating function of the AoI in multi-source systems with computation-intensive status updates," *arXiv preprint arXiv:2102.01126*, 2021.

[6] R. Li, Q. Ma, J. Gong, Z. Zhou, and X. Chen, "Age of processing: Age-driven status sampling and processing offloading for edge computing-enabled real-time IoT applications," *IEEE Internet Things J.*, 2021.

[7] C. Xu, H. H. Yang, X. Wang, and T. Q. Quek, "Optimizing information freshness in computing-enabled IoT networks," *IEEE Internet Things J.*, vol. 7, no. 2, pp. 971–985, 2019.

[8] A. Arafa, R. D. Yates, and H. V. Poor, "Timely cloud computing: Preemption and waiting," in *Proc. of IEEE Annual Allerton Conference on Communication, Control, and Computing (Allerton)*. Monticello, IL, USA: IEEE, Sep. 2019.

[9] B. Buyukates and S. Ulukus, "Timely distributed computation with stragglers," *IEEE Trans. Commun.*, vol. 68, no. 9, pp. 5273–5282, 2020.

[10] S. Kaul, R. Yates, and M. Gruteser, "Real-time status: How often should one update?" in *Proc. of IEEE International Conference on Computer Communications (INFOCOM)*, Orlando, FL, USA, March 2012.

[11] Y. Sun, E. Uysal-Biyikoglu, R. D. Yates, C. E. Koksal, and N. B. Shroff, "Update or wait: How to keep your data fresh," *IEEE Trans. Inf. Theory*, vol. 63, no. 11, pp. 7492–7508, Nov 2017.

[12] Y. Wu, X. Gao, S. Zhou, W. Yang, Y. Polyanskiy, and G. Caire, "Massive access for future wireless communication systems," *IEEE Wireless Commun.*, vol. 27, no. 4, pp. 148–156, Aug. 2020.

[13] H. H. Yang, C. Xu, X. Wang, D. Feng, and T. Q. Quek, "Understanding age of information in large-scale wireless networks," *arXiv preprint arXiv:2012.12472*, 2020.

[14] B. Zhou and W. Saad, "Performance analysis of age of information in ultra-dense internet of things (IoT) systems with noisy channels," *arXiv preprint arXiv:2012.05109*, 2020.

[15] ——, "Age of information in ultra-dense IoT systems: Performance and mean-field game analysis," *arXiv preprint arXiv:2006.15756*, 2020.

[16] D. Narasimha, S. Shakkottai, and L. Ying, "A mean field game analysis of distributed MAC in ultra-dense multichannel wireless networks," in *Proc. of ACM International Symposium on Mobile Ad Hoc Networking and Computing (Mobihoc)*, Catania, Italy, July 2019, pp. 1–10.

[17] A. Maatouk, M. Assaad, and A. Ephremides, "On the age of information in a CSMA environment," *IEEE/ACM Trans. Netw.*, vol. 28, no. 2, pp. 818–831, April 2020.

[18] R. D. Yates and S. K. Kaul, "The age of information: Real-time status updating by multiple sources," *IEEE Trans. Inf. Theory*, vol. 65, no. 3, pp. 1807–1827, March 2019.

[19] N. Gast, "Expected values estimated via mean-field approximation are 1/N-accurate," *Proc. ACM Meas. Anal. Comput. Syst.*, vol. 1, no. 1, June 2017.

[20] L. Ying, "On the approximation error of mean-field models," *SIGMETRICS Perform. Eval. Rev.*, vol. 44, no. 1, p. 285–297, Jun. 2016.

[21] L. Bortolussi and N. Gast, *Mean-Field Limits Beyond Ordinary Differential Equations*. Cham: Springer International Publishing, 2016, pp. 61–82.

[22] L. Jiang and J. Walrand, "A distributed CSMA algorithm for throughput and utility maximization in wireless networks," *IEEE/ACM Trans. Netw.*, vol. 18, no. 3, pp. 960–972, June 2010.

[23] B. Li and A. Eryilmaz, "Optimal distributed scheduling under time-varying conditions: A fast-csma algorithm with applications," *IEEE Trans. Wireless Commun.*, vol. 12, no. 7, pp. 3278–3288, 2013.

[24] N. Bouman, S. Borst, and J. van Leeuwaarden, "Achievable delay performance in csma networks," in *Proc. of IEEE Annual Allerton Conference on Communication, Control, and Computing (Allerton)*. Monticello, IL, USA: IEEE, 2011.

[25] M. Costa, M. Codreanu, and A. Ephremides, "On the age of information in status update systems with packet management," *IEEE Trans. Inf. Theory*, vol. 62, no. 4, pp. 1897–1910, 2016.

[26] J. Cho, J. Le Boudec, and Y. Jiang, "On the asymptotic validity of the decoupling assumption for analyzing 802.11 MAC protocol," *IEEE Trans. Inf. Theory*, vol. 58, no. 11, pp. 6879–6893, Nov. 2012.

ISBN 978-3-903176-37-9 © 2021 IFIP